Detection of OH Stretching Mode of CH₃OH Chemisorbed on Ni₃⁺ and Ni₄⁺ by Infrared Photodissociation Spectroscopy†

Shinichi Hirabayashi

East Tokyo Laboratory, Genesis Research Institute, Inc., 717-86 Futamata, Ichikawa, Chiba 272-0001, Japan

Ryuji Okawa

Graduate School of Science and Engineering, Chuo University, 1-13-27 Kasuga, Bunkyo-ku, Tokyo 112-8551, Japan

Masahiko Ichihashi and Tamotsu Kondow*

Cluster Research Laboratory, Toyota Technological Institute, 717-86 Futamata, Ichikawa, Chiba 272-0001, Japan

Yoshiyuki Kawazoe

Institute for Materials Research, Tohoku University, 2-1-1 Katahira, Aoba-ku, Sendai 980-8577, Japan

Structures of nickel cluster ions adsorbed with methanol, $Ni_3^+(CH_3OH)_m$ ($m = 1-3$) and $Ni_4^+(CH_3OH)_m$ ($m = 1-4$) were investigated by using infrared photodissociation (IR-PD) spectroscopy based on a tandem-type mass spectrometer, where they were produced by passing $Ni_{3,4}^+$ through methanol vapor under a multiple collision condition. The IR-PD spectra were measured in the wavenumber region between 3100 and 3900 cm^{-1}. In each IR-PD spectrum, a single peak was observed at a wavenumber lower by $\sim$40 cm^{-1} than that of the OH stretching vibration of a free methanol molecule and was assigned to the OH stretching vibrations of the methanol molecules in $Ni_{3,4}^+(CH_3OH)_m$. The photodissociation was analyzed by assuming that $Ni_{3,4}^+(CH_3OH)_m$ dissociate unimolecularly after the photon energy absorbed by them is statistically distributed among the accessible modes of $Ni_{3,4}^+(CH_3OH)_m$. In comparison with the calculations performed by the density functional theory, it is concluded that (1) the oxygen atom of each methanol molecule is bound to one of the nickel atoms in $Ni_{3,4}^+$ (defined as molecular chemisorption), (2) the methanol molecules in $Ni_{3,4}^+(CH_3OH)_m$ do not form any hydrogen bonds, and (3) the cross section for demethanation [CH_4 detachment from $Ni_n^+(CH_3OH)$] is related to the electron density distribution inside the methanol molecule.

1. Introduction

It has been reported that transition metal clusters react with molecules in the gas phase, and the reactivity depends characteristically on the size of the cluster.[1,2] In principle, the reaction rate is closely related to the electronic and the geometric structures, as shown by the finding that the size-dependency of the relative reaction rate correlates well with that of the electronic properties such as the ionization potential[3,4] and the HOMO−LUMO gap.[5,6] Needless to say, the reaction itself changes with the cluster size as well. For instance, size-specific reactions of Ni_n^+ with simple molecules have been reported by several groups.[7−12] Irion and Selinger have investigated size-selected Ni_n^+ ($n = 2-20$) with ethylene by using a Fourier transform ion cyclotron resonance (FTICR) mass spectrometer.[7] They have revealed that Ni_n^+ ($n = 2, 5-20$) reacts with C_2H_4 into $Ni_n^+(C_2H_2)_m$, whereas $Ni_{3,4}^+$ is nonreactive. Wöste and co-workers have reported similar size-specific reactions of Ni_n^+ ($n = 4-31$) with carbon monoxide under multiple collision conditions; carbide formation, $Ni_n^+C(CO)_m$ was observed only

in the Ni_n^+ with $n = 4-6$.[9,10] Our recent study on the reaction of Ni_n^+ ($n = 3-11$) with a methanol molecule under single collision conditions has shown that demethanation proceeds preferentially on Ni_4^+, carbide formation on $Ni_{7,8}^+$, and chemisorption on Ni_6^+.[11] The subsequent theoretical study on the same reaction has elucidated that the reactivity (cross section and branching fraction) correlates to the HOMO−LUMO gap and the d-vacancy (the number of d-holes per atom).[13]

All of these experimental studies deal mainly with detection and identification of the initial and final products by mass analysis, without any knowledge of intermediate species, the interaction and bonding between the metal clusters and adsorbates, etc. For furthering the mechanistic investigation of the reactions, infrared photodissociation (IR-PD) spectroscopy is a powerful method because it provides structural information on the chemical species involved in the reactions. Recently, this approach using a free electron laser has been applied to observations of chemical species emerging in the course of reactions.[14−21] Chemical species in the reactions of clusters of Fe, Cu, Ag, and Au with methanol molecules have also been observed by IR-PD spectroscopy in the region of the CO stretching vibration.[22−28] These studies have shown that mo-
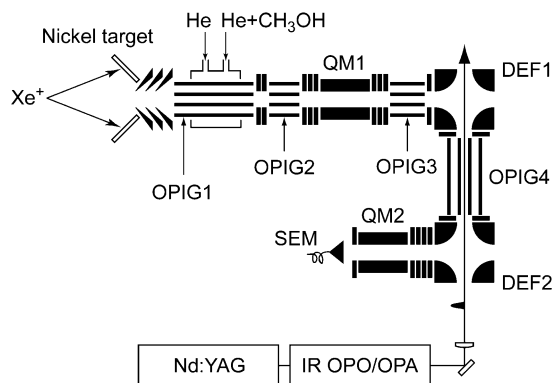

Figure 1. Schematic diagram of the experimental apparatus employed: OPIG, octopole ion guide; QM, quadrupole mass filter; DEF, quadrupole ion deflector; SEM, secondary electron multiplier.

lecularly chemisorbed methanol is formed on the metal clusters when they are allowed to collide with methanol. In addition, the profiles of the IR-PD spectra indicate that the molecularly chemisorbed methanol molecules interact weakly with one another,[25−28] except for them on the Fe cluster.[24]

In this study, Ni$_n^+$(CH$_3$OH)$_m$ were produced by the reaction of nickel cluster ions with methanol in the gas phase, and were identified by using IR-PD spectroscopy based on a tandem-type mass spectrometer. The IR-PD spectra of Ni$_n^+$(CH$_3$OH)$_m$ (n = 3, 4; $m \leq n$) were measured in the wavenumber region of the OH stretching vibration of methanol molecules. The spectra thus measured were assigned with the aid of the density functional theory (DFT). It was found that each methanol molecule is bound to one of the nickel atoms in Ni$_n^+$ through the oxygen atom without forming hydrogen bonds among the methanol molecules.

2. Experimental Section

A part of the apparatus employed in the present study has been reported in our previous paper,[11] so that the equipments modified particularly for the present study are described here. The experimental apparatus consists of an ion source, a tandem-type mass spectrometer, and an IR OPO/OPA laser, as shown schematically in Figure 1. Nickel cluster ions were produced by sputtering onto four separate nickel targets (Nilaco, 99.7% in purity) by Xe$^+$ from an ion gun (CORDIS Ar25/35c, Rokion Ionenstrahl-Technologie). Sputtered cluster ions were introduced into the first octopole ion beam guide (OPIG) mounted in a cooling cell filled with a mixture of helium gas and methanol vapor at 300 K with the volume ratio of 100:1. A total pressure of the gas mixture was ~10^{-3} Torr. Methanol-adsorbed species, Ni$_n^+$(CH$_3$OH)$_m$, were mass-selected by the first quadrupole mass filter (162-8, Extrel) after passing through the second OPIG. The mass-selected parent ions were transported through the third OPIG and deflected at a right angle by the first quadrupole ion deflector into the fourth OPIG, in which the cluster ions interact with an infrared laser introduced coaxially with the fourth OPIG. Intact and fragment ions from the fourth OPIG were deflected perpendicularly by the second quadrupole ion deflector. The fragment ions, Ni$_n^+$(CH$_3$OH)$_{m-1}$, were allowed to pass through the second quadrupole mass filter and were detected by a secondary electron multiplier (Channeltron, 4139S, Burle). Signals from the detector were processed in a pulse counting mode. An IR OPO/OPA (LaserVision) pumped by an injection-seeded Nd:YAG laser (Continuum, SureliteIII) was used for photodissociation at the repetition rate of 10 Hz. The infrared laser beam was loosely focused into the center of
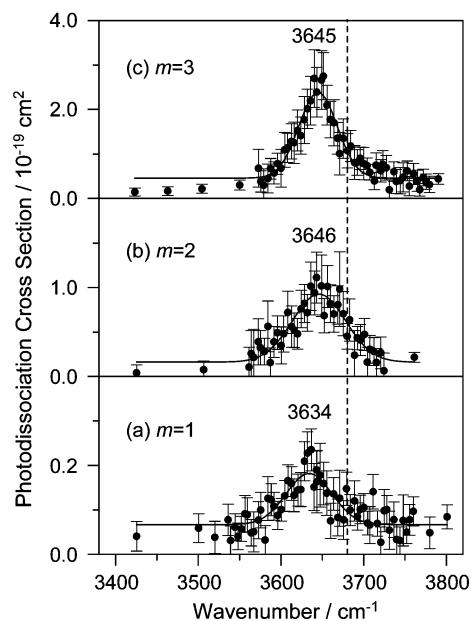
Figure 2. IR-PD spectra of Ni$_3^+$(CH$_3$OH)$_m$ (m = 1−3). The peak frequencies are determined by fitting a Gaussian function to the experimental data. The dashed line indicates the frequency of the OH stretching mode for a free methanol molecule (3681 cm^{-1}).

the second quadrupole ion deflector with a CaF$_2$ lens having a 600 mm focal length. A typical pulse energy was 1−3 mJ/pulse.

An IR-PD spectrum was obtained by measuring photodissociation cross sections as a function of the laser wavenumber. Because the cluster ion beam is overlapped within the infrared laser beam, an absolute photodissociation cross section, σ, was obtained from

$$\sigma = \frac{\pi r^2 h\nu}{Q} \ln \frac{I_0}{I_0 - I} \tag{1}$$

where r is the radius of the laser beam, $h\nu$ is the photon energy, Q is the pulse energy of the laser, and I_0 and I represent the intensities of the parent cluster ion and the given fragment ion due to laser irradiation, respectively. The photodissociation in the present experiment is considered to be a single photon process, because the infrared laser is unfocused in the interaction region. The intensity of the fragment ions, I, was measured in the following procedure: The data acquisition was started at a time when the flashlamp of the YAG laser was triggered, and was performed serially with time windows of 50 μs. The background signal due to unimolecular dissociation was observed. This dissociation ratio was typically 1% of the parent ions. The signal due to photodissociation was measured at ~400 μs after the start of data acquisition with a duration time of typically 100 μs, which corresponds to the residence time of the cluster ions in the forth OPIG. Each data point was obtained by accumulation of 5000−10000 laser pulses, so as to obtain reliable data with S/N of more than 5 near the peak frequencies.

3. Results

Figure 2 shows the IR-PD spectra of Ni$_3^+$(CH$_3$OH)$_m$ (m = 1−3) in the 3400−3800 cm^{-1} region. The measured spectra are reproduced well by a single Gaussian function. The peak frequencies and intensities thus determined are summarized in Table 1. The spectrum of Ni$_3^+$(CH$_3$OH) shows the peak at 3634 cm^{-1}, which is slightly red-shifted from that of a free methanol molecule (3681 cm^{-1}),[29] as shown in Figure 2a. Similar red-

TABLE 1: Measured and Calculated Frequencies, ν (cm^{-1}), and Integrated Intensities, S (km/mol), for Ni$_3^+$(CH$_3$OH)$_m$ (m = 1−3) and Ni$_4^+$(CH$_3$OH)$_m$ (m = 1−4)^a

	experiment		calculation		
species	ν_{exp}	S_D	ν_{calc}	S_A	$S_D/\Sigma S_A$ (%)
CH$_3$OH	3681^b		3681	22.0	
Ni$_3^+$(CH$_3$OH)	3634(3)	4.8	3640	125.9	3.8
Ni$_3^+$(CH$_3$OH)$_2$	3646(2)	37.1	3650	26.7	18.2
			3651	177.6	
Ni$_3^+$(CH$_3$OH)$_3$	3645(1)	67.5	3650	78.9	25.5
			3653	100.3	
			3654	85.5	
Ni$_4^+$(CH$_3$OH)	3645(11)	21.4	3666	111.6	19.2
Ni$_4^+$(CH$_3$OH)$_2$	3642(6)	22.3			
Ni$_4^+$(CH$_3$OH)$_3$	3639(6)	77.5			
Ni$_4^+$(CH$_3$OH)$_4$	3638(3)	80.3			

^{a} The measured peak frequencies, ν_{exp}, and photodissociation intensities, S_D, are determined by fitting a Gaussian function to the experimental data. Standard deviations are given in parentheses. The calculated frequencies are scaled by a factor of 0.983. The values of a free methanol molecule are given for comparison. ^{b} Reference 29.
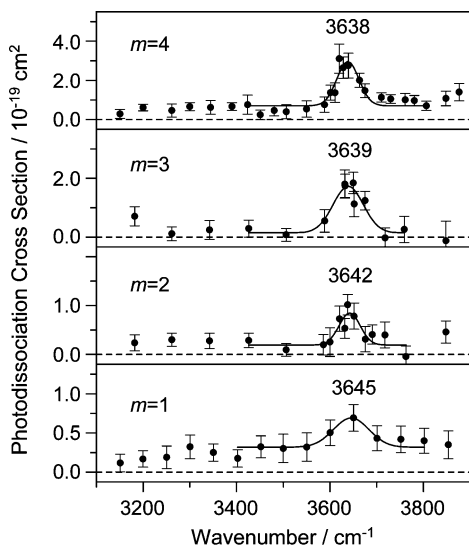
Figure 3. IR-PD spectra of Ni$_4^+$(CH$_3$OH)$_m$ (m = 1−4). The peak frequencies are determined by fitting a Gaussian function to the experimental data.

shifts have been reported for Cs$^+$(CH$_3$OH) and Mg$^+$(CH$_3$OH), where the oxygen atom of the methanol molecule is bonded to the metal ion.[30,31] In comparison with the previous results mentioned above, it is concluded that the measured peak in the spectrum of Ni$_3^+$(CH$_3$OH) originates from the OH stretching vibration of CH$_3$OH adsorbed on Ni$_3^+$ through the oxygen atom.

As shown in Figure 2b,c, the peaks of the Ni$_3^+$(CH$_3$OH)$_{2,3}$ spectra are blue-shifted by ∼10 cm^{-1} with respect to that of the Ni$_3^+$(CH$_3$OH) spectrum, and the photodissociation cross sections increase with the number of the adsorbed methanol molecules. No peak was observed in the region below 3600 cm^{-1}, in which the hydrogen-bonded OH stretching vibration has been reported to be present in the spectra of small methanol clusters.[32−34] These findings indicate that the metal−methanol interactions are more dominant than the methanol−methanol interaction; that is, each methanol molecule is likely to attach individually to one nickel atom of the nickel cluster ions. Similarly, it has been reported that there is no interaction between the adsorbed methanol molecules on neutral iron clusters.[24]

Figure 3 shows the IR-PD spectra of Ni$_4^+$(CH$_3$OH)$_m$ (m = 1−4) measured in the 3100−3900 cm^{-1} region. These spectra
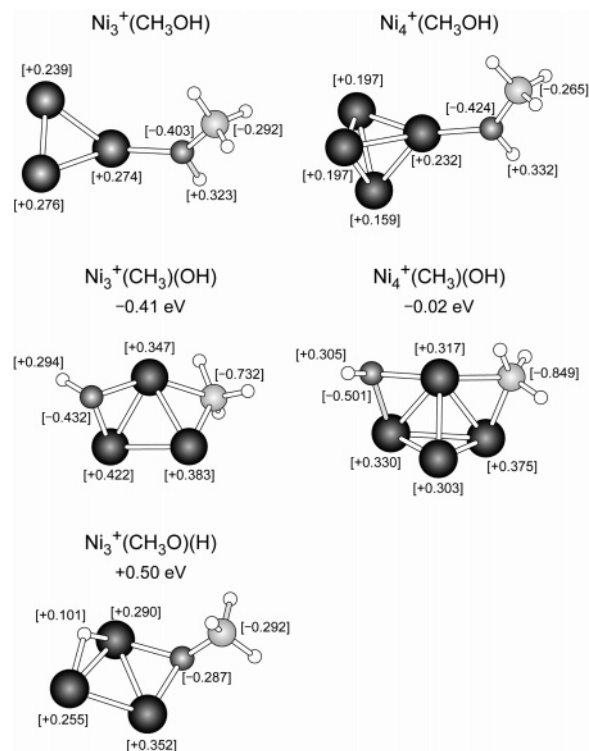
Figure 4. Optimized structures of Ni$_3^+$(CH$_3$OH), Ni$_3^+$(CH$_3$)(OH), Ni$_3^+$-(CH$_3$O)(H), Ni$_4^+$(CH$_3$OH), and Ni$_4^+$(CH$_3$)(OH) determined by BPW91/6-311+G(d,p) calculations. Mulliken atomic charges are given in square brackets. Relative energies are shown with respect to the energy of Ni$_n^+$(CH$_3$OH).

exhibit a single peak near 3640 cm^{-1}, but no peak assignable to the hydrogen bonding is present. Unlike the spectra of Ni$_3^+$(CH$_3$OH)$_m$ (m = 1−3), we cannot detect any difference among the peak frequencies of the OH stretching vibration in the spectra of Ni$_4^+$(CH$_3$OH)$_m$ (m = 1−4), because of insufficient statistics of the data acquisition. Table 1 lists the peak frequencies and intensities.

4. Calculation

DFT calculations were performed by using the GAUSSIAN 98 program package.[35] The structures of Ni$_3^+$(CH$_3$OH)$_m$ (m = 1−3), Ni$_3^+$(CH$_3$)(OH), Ni$_3^+$(CH$_3$O)(H), Ni$_4^+$(CH$_3$OH), and Ni$_4^+$(CH$_3$)(OH) were fully optimized by use of the Becke exchange functional and Perdew and Wang's 1991 gradient-correlated correction functional (BPW91)[36,37] with the 6-311+G-(d,p) basis set. In these calculations, Ni$_3^+$ and Ni$_4^+$ were assumed to have triangle and tetrahedral structures, respectively, with the spin multiplicity of 4. These structures and spin multiplicities were found to be energetically favorable in our previous DFT calculation.[13] The structural optimization of Ni$_n^+$(CH$_3$OH) (n = 3, 4) was performed by assuming that the oxygen atom of the methanol molecule is bound to Ni$_n^+$. In structure optimization of Ni$_3^+$(CH$_3$OH)$_{2,3}$, we used the initial structures in which each methanol molecule is adsorbed on the different nickel atom of the cluster ions. The harmonic vibrational frequencies and the IR absorption intensities were also calculated for the comparison with the measured values.

5. Discussion

5.1. Structures and Vibrational Frequencies. Figures 4 and 5 illustrate the optimized structures of Ni$_3^+$(CH$_3$OH)$_m$ with m = 1−3 and Ni$_4^+$(CH$_3$OH). The structural parameters and adsorption energies of CH$_3$OH onto Ni$_n^+$ are listed in Table 2,

OH Stretching Mode of CH₃OH on Ni$_n^+$

J. Phys. Chem. A, Vol. 111, No. 31, 2007 **7667**
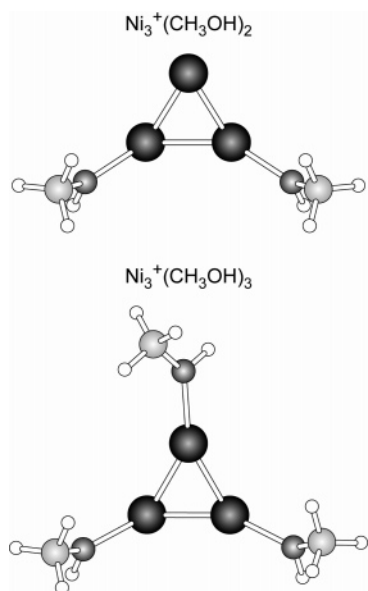
Figure 5. Optimized structures of Ni$_3^+$(CH$_3$OH)$_2$ and Ni$_3^+$(CH$_3$OH)$_3$ determined by BPW91/6-311+G(d,p) calculations.

TABLE 2: Calculated Bond Lengths (Å) and Adsorption Energies, $V_{n,m}$ (eV), of CH₃OH onto Ni$_n^+$ for Ni$_3^+$(CH$_3$OH)$_m$ (m = 1−3) and Ni$_4^+$(CH$_3$OH)^a

species	Ni−O	O−H	C−O	$V_{n,m}$
CH₃OH		0.969	1.431	
Ni$_3^+$(CH$_3$OH)	1.967	0.973	1.470	1.48
Ni$_3^+$(CH$_3$OH)$_2$	1.987	0.972	1.466	1.36
	1.987	0.972	1.466	
Ni$_3^+$(CH$_3$OH)$_3$	2.004	0.972	1.462	1.25
	2.010	0.972	1.461	
	2.012	0.972	1.461	
Ni$_4^+$(CH$_3$OH)	1.975	0.971	1.468	1.31

^{a} The bond lengths of a free methanol molecule are given for comparison.

together with the corresponding values of a free methanol molecule. The calculated harmonic frequencies are scaled by a factor of 0.983, because the OH stretching frequency of a free methanol molecule is calculated to be larger by a factor of 0.983^{-1} than the experimental one. The calculated frequencies thus obtained are compared with the experimental ones in Table 1.

In Ni$_3^+$(CH$_3$OH), the oxygen atom of CH₃OH is bound to the on-top site of Ni$_3^+$. Similar on-top geometries have been suggested for methanol molecules on gold cluster ions.[38] In the present calculation, we attempted to optimize for other adsorption sites such as a bridge site and found that the on-top site is the most favorable one. The adsorption energy of Ni$_3^+$(CH$_3$-OH) was calculated to be 1.48 eV, which is larger than the chemisorption energy on an Ni(110) surface, 0.6 eV [14 ± 4 kcal/mol].[39,40] These findings lead us to conclude that CH₃OH in Ni$_3^+$(CH$_3$OH) is chemically adsorbed to Ni$_3^+$. All the methanol molecules of Ni$_3^+$(CH$_3$OH)$_{2,3}$ are preferably bound to the on-top sites as well. The averaged adsorption energies per one methanol molecule for Ni$_3^+$(CH$_3$OH)$_m$ with m = 2 and 3 were calculated to be 1.36 and 1.25 eV, respectively, which are smaller than that for Ni$_3^+$(CH$_3$OH). In Ni$_3^+$(CH$_3$OH)$_m$ (m = 1−3), the length of the Ni−O bond increases and the adsorption energy decreases as m increases. (see Table 2). The C−O and the O−H bond lengths, which are larger than those of an isolated methanol molecule, decrease slightly with the increase of m. In Ni$_4^+$(CH$_3$OH), the oxygen atom of the methanol molecule binds to the on-top site of Ni$_4^+$, similarly to the case of Ni$_3^+$(CH$_3$OH) (see Figure 4). There is no

TABLE 3: Mulliken Charges, q, of Ni$_n^+$, OH, and CH₃ in Ni$_n^+$(CH$_3$OH) (n = 3, 4), and Differences of the Charges for a Given Bond^a

species	q(Ni$_n$)	q(OH)	q(CH$_3$)	q(H) − q(O)	q(CH$_3$) − q(OH)
CH₃OH		−0.104	+0.104	+0.599	+0.208
Ni$_3^+$	+1.000				
Ni$_3^+$(CH$_3$OH)	+0.789	−0.080	+0.291	+0.726	+0.371
Ni$_4^+$	+1.000				
Ni$_4^+$(CH$_3$OH)	+0.785	−0.092	+0.308	+0.756	+0.400

^{a} The values of a free methanol molecule and nickel cluster ions are given for comparison.

significant difference between the bond lengths of CH₃OH in Ni$_3^+$(CH$_3$OH) and Ni$_4^+$(CH$_3$OH). The adsorption energy of Ni$_4^+$(CH$_3$OH) was calculated to be 1.31 eV.

As shown in Table 1, all the calculated frequencies of Ni$_n^+$(CH$_3$OH)$_m$ are red-shifted from that of a free methanol molecule. The red shift results from the elongation of the O−H bond. The cluster ions, Ni$_3^+$(CH$_3$OH)$_2$ and Ni$_3^+$(CH$_3$OH)$_3$, have two and three OH stretching vibrational modes, respectively, which are blue-shifted by ~10 cm^{-1} from that of Ni$_3^+$(CH$_3$-OH). The calculated frequencies reproduce well the experimental ones. The agreements support that the structures presented here are reliable.

To evaluate the contribution of the dissociative species, Ni$_n^+$-(CH$_3$)(OH), in the spectra observed, we calculated the optimized structures and their vibrational frequencies of Ni$_n^+$(CH$_3$)(OH) with n = 3 and 4 (see Figure 4). The frequency of the OH stretching vibration of Ni$_3^+$(CH$_3$)(OH) was obtained to be 3596 cm^{-1}, which is much lower than the measured peak frequency of 3634 cm^{-1}. The calculated absorption intensity of this vibrational mode is as high as the calculated one of Ni$_3^+$(CH$_3$-OH). The dissociative species is energetically more stable by 0.4 eV than Ni$_3^+$(CH$_3$-OH). However, no peak assignable to Ni$_3^+$(CH$_3$)(OH) is present in the measured spectrum of Ni$_3^+$(CH$_3$-OH). This finding implies that the energy barrier from Ni$_3^+$(CH$_3$-OH) to Ni$_3^+$(CH$_3$)(OH) is too high for the reaction to proceed. It is concluded that Ni$_3^+$(CH$_3$OH) is much more abundant than Ni$_3^+$(CH$_3$)(OH). On the other hand, Ni$_4^+$(CH$_3$OH) and Ni$_4^+$-(CH$_3$)(OH) have the OH stretching frequencies of 3666 and 3641 cm^{-1}, respectively, which are in good agreement with the measured peak frequency of 3645 cm^{-1}. In addition, the energies of molecularly and dissociatively chemisorbed species differ only by 0.02 eV. It is likely that Ni$_4^+$(CH$_3$)(OH) coexist with Ni$_4^+$(CH$_3$OH) as the reaction products. Photodissociation of Ni$_4^+$(CH$_3$)(OH) following a single IR photon excitation may take place via the recombination of CH₃ and OH on Ni$_4^+$. Separate liberation of CH₃ and OH from Ni$_4^+$(CH$_3$)(OH) is unlikely because the binding energies of CH₃ and OH should be significantly higher than that of CH₃OH.

5.2. Relationship between Chemisorbed Structure with Size-dependent Reactivity. In the reaction of Ni$_4^+$ with a methanol molecule under single collision conditions, a methane molecule is released with leaving Ni$_4$O$^+$ (demethanation), but the demethanation hardly occurs on Ni$_3^+$.[11] The geometrical structure and the site of the chemisorbed CH₃OH on Ni$_4^+$ is almost the same as that of Ni$_3^+$ as described above, but the electron density distributions of the Mulliken charges differ significantly. As shown in Figure 4, Ni$_4^+$(CH$_3$OH) carries a higher negative charge on the O atom and positive charge on the H atom of the hydroxyl group than Ni$_3^+$(CH$_3$OH) does. In addition, the electron density is polarized between CH₃ and OH at a greater extent in Ni$_4^+$(CH$_3$OH) than in Ni$_3^+$(CH$_3$OH) (see Table 3). These findings indicate that the electron density

distribution is closely related to the demethanation that occurs efficiently on Ni_4^+. As mentioned in the previous subsection, the chemisorbed methanol molecule dissociate to $-CH_3$ and $-OH$ on Ni_4^+. Presumably, the demethanation proceeds via $Ni_4^+(CH_3)(OH)$, which is preferentially produced from the polarized CH_3OH on Ni_4^+.

5.3. Interpretation of Photodissociation Cross Section. The calculated integrated photoabsorption intensities (calculated IR absorption intensities) are compared with the measured integrated photodissociation intensities as shown in Table 1. The photodissociation intensities are lower than the photoabsorption ones, because both the photoabsorption and the dissociation probabilities should be taken into account to obtain the photodissociation intensities. In addition, the internal energy of a parent cluster ion should be considered as well.

The internal energy distribution of a parent cluster ion is defined as $P(E)$, which is statistically distributed in the accessible internal modes of the parent cluster ion, where E is the internal energy of the parent cluster ion. Let us assume that the distribution, $P_0(E_{ini})$, of the parent cluster ion having the initial internal energy, E_{ini}, obeys a Gaussian distribution with the peak energy of E_0 and the width of W. The parent ion under irradiation of an IR laser happens to absorb one photon and hence their internal energies increase by the photon energy, $h\nu$. Then, the energy distribution of the parent cluster ion is given by the sum of two Gaussian distributions, $P_A(E_{ini} + h\nu)$ and $P_1(E_{ini})$, where $P_A(E_{ini} + h\nu)$, which has the peak energy of $E_0 + h\nu$ and the width of W, is the energy distribution of the photoexcited parent cluster ion and $P_1(E_{ini})$ is the distribution of an intact parent cluster ion. The relative intensity, $D_{n,m}(E)$, of $Ni_n^+(CH_3OH)_{m-1}$ produced from the dissociation of $Ni_n^+(CH_3OH)_m$ is calculated by

$$D_{n,m}(E) = 1 - \exp\{-k_{n,m}(E)t\} \tag{2}$$

where $k_{n,m}(E)$ is the dissociation rate constant and t is the reaction time. The reaction time is approximated by the flight time ($\sim 250 \mu s$) from the exit of the first quadrupole mass filter to the entrance of the second quadrupole mass filter. The dissociation rate, $k_{n,m}(E)$, is estimated from the Rice–Ramsperger–Kassel (RRK) theory as[41]

$$k_{n,m}(E) = A\left(\frac{E - V_{n,m}}{E}\right)^{L-1} \tag{3}$$

where A is the frequency factor, E is the internal energy, $V_{n,m}$ is the adsorption energy per methanol molecule on Ni_n^+, and L ($= 3n + 6m - 6$) is the number of the vibrational modes in $Ni_n^+(CH_3OH)_m$. In this model, the intramolecular modes of the CH_3OH molecules are excluded because most of the internal energy is statistically distributed into the low vibrational modes. The frequency factor, A, is chosen as $4 \times 10^{12} s^{-1}$, which corresponds to an average of intermolecular vibrational frequencies. The adsorption energies, $V_{n,m}$, employed are listed in Table 2; $V_{n,m}$ were calculated by the DFT method.

Under irradiation of the IR laser used in the present study, it is possible for a parent cluster ion to undergo dissociation even by absorbing one photon with the energy ($h\nu = 0.45$ eV) less than the dissociation energy, because the parent cluster ion has a sufficient initial internal energy. By using eqs 2 and 3, the relative intensity of the photofragment ion was calculated as the difference of the relative intensities, $D_{n,m}(E)$, with and without laser irradiation. The ratio of the photoexcited parent cluster ion was estimated from the calculated integrated photoabsorption intensity.

TABLE 4: Parameters of the Initial Internal Energy Distribution for $Ni_3^+(CH_3OH)_m$ ($m = 1-3$) and $Ni_4^+(CH_3OH)$ Obtained from Unimolecular Decay

species	E_0 (eV)	W (eV)	L	E_0/L (eV)
$Ni_3^+(CH_3OH)$	0.64	0.65	9	0.07
$Ni_3^+(CH_3OH)_2$	1.08	0.54	15	0.07
$Ni_3^+(CH_3OH)_3$	1.32	0.53	21	0.06
$Ni_4^+(CH_3OH)$	0.98	0.42	12	0.08

The measured relative intensities of the fragment ion without laser irradiation and the photofragment ion are reproduced well by the calculated ones (see eqs 2 and 3) by adjusting E_0 and W of the initial internal energy distribution, $P_0(E_{ini})$. The parameters thus obtained for $Ni_3^+(CH_3OH)_m$ ($m = 1-3$) and $Ni_4^+(CH_3-OH)$ are listed in Table 4. The internal energies per vibrational mode (E_0/L) for all the cluster ions studied are almost same. This finding indicates that the parent ions, $Ni_n^+(CH_3OH)_m$, have a similar probability distribution of the initial internal energy. It follows that the species having higher internal energies dissociate after the photoabsorption and hence contribute to the measured IR-PD spectra.

5.4. Comparison with Bulk Surface. It has been reported that a methanol molecule is dissociatively chemisorbed on a Ni surface into $-OCH_3$ and $-H$ in the temperature range of $140-240$ K.[42] As the temperature increases, the methoxy group decomposes further and leaves from the surface as a carbon monoxide molecule and a hydrogen molecule. On the other hand, methanol molecules adsorb molecularly onto Ni_3^+ and Ni_4^+ at ~ 300 K, as shown in the present study. The measured and calculated adsorption energies of a methanol molecule on a Ni surface are 0.6[40] and 0.2 eV,[43] respectively, which is much lower than that of a methanol molecule on Ni_3^+. Also, the dissociative species, $Ni_3^+(CH_3O)(H)$ (see Figure 4) has the energy that is higher by 0.5 eV than $Ni_3^+(CH_3OH)$, consistent with the result that $Ni_3^+(CH_3OH)$ is detected experimentally. On the other hand, the theoretical study has shown that the dissociative adsorption of $-H$ and $-OCH_3$ on Ni(111) is energetically more stable than the molecular adsorption.[43]

The vibrational spectra of chemisorbed methanol prior to the condensation of multilayer on a bulk nickel surface have been measured by high-resolution electron energy loss spectroscopy.[39,44] The peaks observed at 3215 cm^{-1} on Ni(111)[44] and at 3210 cm^{-1} on Ni(110)[39] were assigned to the OH stretching vibrational mode, which are largely red-shifted from those of $Ni_{3,4}^+(CH_3OH)_m$ studied here. As mentioned in refs 39 and 44, the large red shift is likely to result from the hydrogen bonding between the methanol molecules on the bulk surface or the interaction between a surface metal atom and the hydrogen atom in the hydroxyl group of CH_3OH. Note that no peak is present in the vicinity of ~ 3200 cm^{-1} in the IR-PD spectra of $Ni_{3,4}^+(CH_3OH)_m$.

6. Conclusions

IR-PD spectroscopy was employed to investigate collisional reactions of nickel cluster ions, Ni_n^+ ($n = 3, 4$), with methanol molecules in the gas phase. It is concluded that the methanol molecules are molecularly chemisorbed on Ni_3^+ and the dissociatively chemisorbed species may exist as $-CH_3$ and $-OH$ together with molecularly chemisorbed CH_3OH on Ni_4^+. It is plausible that the specific size-dependent reactivity is determined by the charge distributions of the molecularly chemisorbed CH_3-OH. It is likely that the demethanation proceeds via formation of a reaction intermediate, $Ni_4^+(CH_3)(OH)$; the formation is initiated by polarization induced inside the molecularly chemisorbed CH_3OH on Ni_4^+.

References and Notes

(1) Knickelbein, M. B. *Annu. Rev. Phys. Chem.* **1999**, *50*, 79.

(2) Armentrout, P. B. *Annu. Rev. Phys. Chem.* **2001**, *52*, 423.

(3) Whetten, R. L.; Cox, D. M.; Trevor, D. J.; Kaldor, A. *Phys. Rev. Lett.* **1985**, *54*, 1494.

(4) Whetten, R. L.; Zakin, M. R.; Cox, D. M.; Trevor, D. J.; Kaldor, A. *J. Chem. Phys.* **1986**, *85*, 1697.

(5) Conceicao, J.; Laaksonen, R. T.; Wang, L.-S.; Guo, T.; Nordlander, P.; Smalley, R. E. *Phys. Rev. B* **1995**, *51*, 4668.

(6) Kietzmann, H.; Morenzin, J.; Bechthold, P. S.; Ganteför, G.; Eberhardt, W. *J. Chem. Phys.* **1998**, *109*, 2275.

(7) Irion, M. P.; Selinger, A. *Ber. Bunsen-Ges. Phys. Chem.* **1989**, *93*, 1408.

(8) Irion, M. P.; Schnabel, P.; Selinger, A. *Ber. Bunsen-Ges. Phys. Chem.* **1990**, *94*, 1291.

(9) Fayet, P.; McGlinchey, M. J.; Wöste, L. H. *J. Am. Chem. Soc.* **1987**, *109*, 1733.

(10) Vajda, Š.; Wolf, S.; Leisner, T.; Busolt, U.; Wöste, L. H.; Wales, D. J. *J. Chem. Phys.* **1997**, *107*, 3492.

(11) Ichihashi, M.; Hanmura, T.; Yadav, R. T.; Kondow, T. *J. Phys. Chem. A* **2000**, *104*, 11885.

(12) Hanmura, T.; Ichihashi, M.; Kondow, T. *J. Phys. Chem. A* **2002**, *106*, 4525.

(13) Yadav, R. T.; Ichihashi, M.; Kondow, T. *J. Phys. Chem. A* **2004**, *108*, 7188.

(14) Simard, B.; Dénommée, S.; Rayner, D. M.; van Heijnsbergen, D.; Meijer, G.; von Helden, G. *Chem. Phys. Lett.* **2002**, *357*, 195.

(15) Fielicke, A.; von Helden, G.; Meijer, G.; Simard, B.; Dénommée, S.; Rayner, D. M. *J. Am. Chem. Soc.* **2003**, *125*, 11184.

(16) Fielicke, A.; von Helden, G.; Meijer, G.; Pedersen, D. B.; Simard, B.; Rayner, D. M. *J. Phys. Chem. B* **2004**, *108*, 14591.

(17) Jaeger, T. D.; Fielicke, A.; von Helden, G.; Meijer, G.; Duncan, M. A. *Chem. Phys. Lett.* **2004**, *392*, 409.

(18) Fielicke, A.; von Helden, G.; Meijer, G.; Pedersen, D. B.; Simard, B.; Rayner, D. M. *J. Am. Chem. Soc.* **2005**, *127*, 8416.

(19) Fielicke, A.; von Helden, G.; Meijer, G.; Simard, B.; Rayner, D. M. *Phys. Chem. Chem. Phys.* **2005**, *7*, 3906.

(20) Fielicke, A.; von Helden, G.; Meijer, G.; Simard, B.; Rayner, D. M. *J. Phys. Chem. B* **2005**, *109*, 23935.

(21) Fielicke, A.; von Helden, G.; Meijer, G.; Pedersen, D. B.; Simard, B.; Rayner, D. M. *J. Chem. Phys.* **2006**, *124*, 194305.

(22) Zakin, M. R.; Brickman, R. O.; Cox, D. M.; Reichmann, K. C.; Trevor, D. J.; Kaldor, A. *J. Chem. Phys.* **1986**, *85*, 1198.

(23) Knickelbein, M. B. *Chem. Phys. Lett.* **1995**, *239*, 11.

(24) Knickelbein, M. B. *J. Chem. Phys.* **1996**, *104*, 3517.

(25) Dietrich, G.; Dasgupta, K.; Krückeberg, S.; Lützenkirchen, K.; Schweikhard, L.; Walther, C.; Ziegler, J. *Chem. Phys. Lett.* **1996**, *259*, 397.

(26) Knickelbein, M. B.; Koretsky, G. M. *J. Phys. Chem. A* **1998**, *102*, 580.

(27) Rousseau, R.; Dietrich, G.; Krückeberg, S.; Lützenkirchen, K.; Marx, D.; Schweikhard, L.; Walther, C. *Chem. Phys. Lett.* **1998**, *295*, 41.

(28) Dietrich, G.; Krückeberg, S.; Lützenkirchen, K.; Schweikhard, L.; Walther, C. *J. Chem. Phys.* **2000**, *112*, 752.

(29) Shimanouchi, T. *Tables of Molecular Vibrationl Frequencies*; National Bureau of Standards Reference Data Series; NBS: Washington, DC, 1972; Vol. I.

(30) Weinheimer, C. J.; Lisy, J. M. *Int. J. Mass. Spectrom. Ion Processes* **1996**, *159*, 197.

(31) Machinaga, H.; Ohashi, K.; Inokuchi, Y.; Nishi, N.; Sekiya, H. *Chem. Phys. Lett.* **2004**, *391*, 85.

(32) Huisken, F.; Kulcke, A.; Laush, C.; Lisy, J. M. *J. Chem. Phys.* **1991**, *95*, 3924.

(33) Huisken, F.; Kaloudis, M.; Koch, M.; Werhahn, O. *J. Chem. Phys.* **1996**, *105*, 8965.

(34) Provencal, R. A.; Paul, J. B.; Roth, K.; Chapo, C.; Casaes, R. N.; Saykally, R. J.; Tschumper, G. S.; Schaefer, H. F., III. *J. Chem. Phys.* **1999**, *110*, 4258.

(35) Frisch, M. J.; Trucks, G. W.; Schlegel, H. B.; Scuseria, G. E.; Robb, M. A.; Cheeseman, J. R.; Zakrzewski, V. G.; Montgomery, J. A., Jr.; Stratmann, R. E.; Burant, J. C.; Dapprich, S.; Millam, J. M.; Daniels, A. D.; Kudin, K. N.; Strain, M. C.; Farkas, O.; Tomasi, J.; Barone, V.; Cossi, M.; Cammi, R.; Mennucci, B.; Pomelli, C.; Adamo, C.; Clifford, S.; Ochterski, J.; Petersson, G. A.; Ayala, P. Y.; Cui, Q.; Morokuma, K.; Salvador, P.; Dannenberg, J. J.; Malick, D. K.; Rabuck, A. D.; Raghavachari, K.; Foresman, J. B.; Cioslowski, J.; Ortiz, J. V.; Baboul, A. G.; Stefanov, B. B.; Liu, G.; Liashenko, A.; Piskorz, P.; Komaromi, I.; Gomperts, R.; Martin, R. L.; Fox, D. J.; Keith, T.; Al-Laham, M. A.; Peng, C. Y.; Nanayakkara, A.; Challacombe, M.; Gill, P. M. W.; Johnson, B.; Chen, W.; Wong, M. W.; Andres, J. L.; Gonzalez, C.; Head-Gordon, M.; Replogle, E. S.; Pople, J. A. *Gaussian 98*, revision A.11.1; Gaussian, Inc.: Pittsburgh, PA, 2001.

(36) Becke, A. D. *Phys. Rev. A* **1988**, *38*, 3098.

(37) Perdew, J. P.; Wang, Y. *Phys. Rev. B* **1992**, *45*, 13244.

(38) Rousseau, R.; Marx, D. *J. Chem. Phys.* **2000**, *112*, 761.

(39) Bare, S. R.; Stroscio, J. A.; Ho, W. *Surf. Sci.* **1985**, *150*, 399.

(40) Richter, L. J.; Ho, W. *J. Chem. Phys.* **1985**, *83*, 2569.

(41) Draves, J. A.; Luthey-Schulten, Z.; Liu, W.-L.; Lisy, J. M. *J. Chem. Phys.* **1990**, *93*, 4589.

(42) Vajo, J. J.; Campbell, J. H.; Becker, C. H. *J. Phys. Chem.* **1991**, *95*, 9457.

(43) Wang, G.-C.; Zhou, Y.-H.; Morikawa, Y.; Nakamura, J.; Cai, Z.-S.; Zhao, X.-Z. *J. Phys. Chem. B* **2005**, *109*, 12431.

(44) Demuth, J. E.; Ibach, H. *Chem. Phys. Lett.* **1979**, *60*, 395.